

## Half-life measurement of short-lived $^{94m}_{44}\text{Ru}^{44+}$ using isochronous mass spectrometry

Q. Zeng,<sup>1,2</sup> M. Wang,<sup>2,\*</sup> X. H. Zhou,<sup>2,†</sup> Y. H. Zhang,<sup>2,3</sup> X. L. Tu,<sup>2,4</sup> X. C. Chen,<sup>2</sup> X. Xu,<sup>2</sup> Yu. A. Litvinov,<sup>2,4,5</sup> H. S. Xu,<sup>2</sup> K. Blaum,<sup>4</sup> R. J. Chen,<sup>2</sup> C. Y. Fu,<sup>2,6</sup> Z. Ge,<sup>2</sup> W. J. Huang,<sup>2,7</sup> H. F. Li,<sup>2,6</sup> J. H. Liu,<sup>2,6</sup> B. Mei,<sup>2</sup> P. Shuai,<sup>2</sup> M. Si,<sup>2,6</sup> B. H. Sun,<sup>8</sup> M. Z. Sun,<sup>2,6</sup> Q. Wang,<sup>2,6</sup> G. Q. Xiao,<sup>2</sup> Y. M. Xing,<sup>2</sup> T. Yamaguchi,<sup>9</sup> X. L. Yan,<sup>2</sup> J. C. Yang,<sup>2</sup> Y. J. Yuan,<sup>2</sup> Y. D. Zang,<sup>2</sup> P. Zhang,<sup>2,6</sup> W. Zhang,<sup>2</sup> and X. Zhou<sup>2,6</sup>

<sup>1</sup>Research Center for Hadron Physics, National Laboratory of Heavy Ion Accelerator Facility in Lanzhou and University of Science and Technology of China, Hefei 230026, People's Republic of China

<sup>2</sup>Key Laboratory of High Precision Nuclear Spectroscopy and Center for Nuclear Matter Science, Institute of Modern Physics, Chinese Academy of Sciences, Lanzhou 730000, People's Republic of China

<sup>3</sup>ExtreMe Matter Institute (EMMI), GSI Helmholtzzentrum für Schwerionenforschung, Planckstraße 1, 64291 Darmstadt, Germany

<sup>4</sup>Max-Planck-Institut für Kernphysik, Saupfercheckweg 1, 69117 Heidelberg, Germany

<sup>5</sup>GSI Helmholtzzentrum für Schwerionenforschung, Planckstraße 1, 64291 Darmstadt, Germany

<sup>6</sup>University of Chinese Academy of Sciences, Beijing 000049, People's Republic of China

<sup>7</sup>CSNSM, Université Paris-Sud, CNRS/IN2P3, Université Paris-Saclay, Orsay 91405, France

<sup>8</sup>School of Physics and Nuclear Energy Engineering, Beihang University, Beijing 100191, People's Republic of China

<sup>9</sup>Department of Physics, Saitama University, Saitama 338-8570, Japan

(Received 13 August 2017; revised manuscript received 29 August 2017; published 27 September 2017)

Decay of the  $8^+$  isomer in fully stripped ions  $^{94}\text{Ru}^{44+}$  is observed during its circulation in the experimental Cooler Storage Ring (CSRe) at the Heavy Ion Research Facility in Lanzhou (HIRFL). The  $^{94}\text{Ru}^{44+}$  ions were produced via projectile fragmentation and stored in CSRe tuned into the isochronous ion-optical mode. The timing signals of the ions, passing through a time-of-flight detector, were consecutively registered and used to determine the variation of revolution time as a function of revolution number. A sudden change of the revolution time at a specific revolution was identified as a fingerprint of the  $^{94}\text{Ru}^{44+}$  isomer decay. The isomeric half-life was deduced to be  $102(17) \mu\text{s}$ , which agrees well with the theoretical expectation by blocking the internal conversion decay of the isomer. Our work proved the feasibility of studying decays of short-lived isomers in high atomic charge states using the isochronous mass spectrometry. In addition,  $^{94m}\text{Ru}^{44+}$  represents the shortest-lived nuclear state whose mass has ever been measured directly.

DOI: [10.1103/PhysRevC.96.031303](https://doi.org/10.1103/PhysRevC.96.031303)

**Introduction.** Highly charged ions (HCI) are well-defined quantum systems. Their decay modes and rates might be significantly different from those in neutral atoms [1–12]. Interesting phenomena have been observed in the decays of HCI. Of the most importance are the discovery of the bound-state  $\beta$  decay [2,5,7] and the investigation of orbital electron-capture decay in hydrogen-like and helium-like ions [8,9,11]. These investigations have led to a deeper understanding of not only the nuclear decay mechanisms but also the nucleosynthesis processes since the involved atoms could be highly charged in hot stellar environments [13]. The decay rates of nuclear isomers in HCI can be largely modified because the internal conversion decay branch is hindered or even blocked due to the reduction or absence of orbital electrons. Isomeric decays in bare [4,6], hydrogen-like [12], and other highly-charged ions [1,3] have been studied using various methods. However, experimental data for very short-lived isomeric decays in highly charged ions are very scarce due to the lack of feasible measuring methods.

Measuring the nuclear decay rates of HCI is experimentally challenging because it requires (1) producing highly charged ions, (2) storing them for sufficiently long times, and (3)

sensitively detecting their decays. Heavy ion accelerator facilities and particularly storage-ring-based facilities provide great opportunities to study the decays of HCI [10,14]. Projectile fragmentation or in-flight fission at high energy are suitable nuclear reactions to produce radioactive nuclei, which directly emerge from the target as highly charged or even fully stripped ions. The decays of HCI during the transmission can be studied with conventional magnetic spectrographs [1,3]. Because of the short time for energetic HCI to pass through a spectrometer, this method is only suitable for the decay study of HCIs with half-lives within  $\sim 100$  ns. We note that the resolving power of such spectrometers is not sufficient to directly resolve the nuclides in the ground and isomeric states. Alternatively, the ions can be stored in ion traps [15] or storage rings [16] for long times. Both devices can reach sufficiently high resolving powers to directly resolve isomers from the corresponding ground states. Their decays lead to the change of mass and in some cases also the ionic charge state. The change will cause a variation of their trajectory and the revolution time, which can directly be observed. In the past two decades, the decays of HCI have been extensively studied at ESR in GSI using time-resolved Schottky mass spectrometry (SMS) [17]. In these experiments, the stored ions were cooled with the electron cooler to assure high resolution, which is demanded to distinguish between the precursor and the decay product in the same charge state. The well-established SMS is an ideal

\*wangm@impcas.ac.cn

†zxh@impcas.ac.cn

tool to study the decay of HCIs with half-lives longer than a few seconds [18].

The decay of an isomer in HCI with half-life in the range from microseconds to milliseconds has not ever been investigated due to the limits of the methods discussed above: The half-life is either too long for the magnetic spectrographs [1,3] or too short for SMS since it takes at least several seconds to cool the stored ions down [12,19–21]. Isochronous mass spectrometry (IMS) [22,23] has been well established and employed at the Experimental Storage Ring ESR in GSI Helmholtz Centre for Heavy Ion Research and at the experimental Cooler Storage Ring (CSRe) in Institute of Modern Physics, Chinese Academy of Sciences for mass measurements of short-lived nuclides. A batch of nuclear masses were measured [24–30] and several isomers were discovered [24]. The mass-resolving power of  $\sim 2.5 \times 10^5$  has been achieved in the IMS at CSRe, which is sufficient to resolve low-lying isomers from the ground states. Taking the advantages of the high mass-resolving power and short time measurement, IMS can be used to study the decay of short-lived HCI, particularly isomers.

In this Rapid Communication, we report the first half-life measurement of the short-lived isomer in fully stripped  $^{94}\text{Ru}^{44+}$  ions using IMS at CSRe. This isomer has a half-life of 71(4)  $\mu\text{s}$  in neutral atoms and an excitation energy of 2644(4) keV [31,32]. It is a seniority isomer with spin and parity of  $8^+$ . It decays either through  $\gamma$  cascades or internal conversion to the  $0^+$  ground state. The internal conversion coefficient (ICC) of this isomer was calculated to be 0.335 using BRICC software [33], from which the half-life of the isomer in a fully stripped ion is predicted to be 95(5)  $\mu\text{s}$ .

*Experiment.* The experiment was performed at the Cooler-Storage Ring at the Heavy Ion Research Facility in Lanzhou (HIRFL-CSR) [34]. A 376.42-MeV/u  $^{112}\text{Sn}^{35+}$  beam was extracted from the main cooler-storage ring CSRm and impinged on a  $\sim 10$ -mm-thick  $^9\text{Be}$  target placed at the entrance of the in-flight separator RIBLL2. The projectile fragments were selected by RIBLL2 and a cocktail beam was injected into the experimental cooler-storage ring CSRe for measurements. Similar to the procedure described in Ref. [7], to reduce the transmission of contaminants, RIBLL2 and CSRe were set to different magnetic-rigidity values. RIBLL2 was set to magnetic rigidity  $B\rho = 5.9630\text{ Tm}$  for an optimal transmission of hydrogen-like ions  $^{94}\text{Ru}^{43+}$ . Then the bound electron was stripped off in a 0.2-mm-thick carbon foil at the exit of RIBLL2, thus producing the bare ions  $^{94}\text{Ru}^{44+}$ . The following beam line and CSRe were set to  $B\rho = 5.5294\text{ Tm}$  to optimize the transmission of  $^{94}\text{Ru}^{44+}$  ions.

The revolution times of the circulating ions in the storage ring are related in first-order approximation to their mass-over-charge ratios ( $m/q$ ) via [16,22]

$$\frac{\Delta T}{T} = \frac{1}{\gamma_i^2} \frac{\Delta(m/q)}{(m/q)} - \left(1 - \frac{\gamma^2}{\gamma_i^2}\right) \frac{\Delta v}{v}, \quad (1)$$

where  $v$  and  $\gamma$  are the velocity and the relativistic Lorentz factor, respectively.  $\gamma_i$  is the transition point, which is a setting parameter of the storage ring. According to Eq. (1), the revolution times of the ions are independent of the velocities

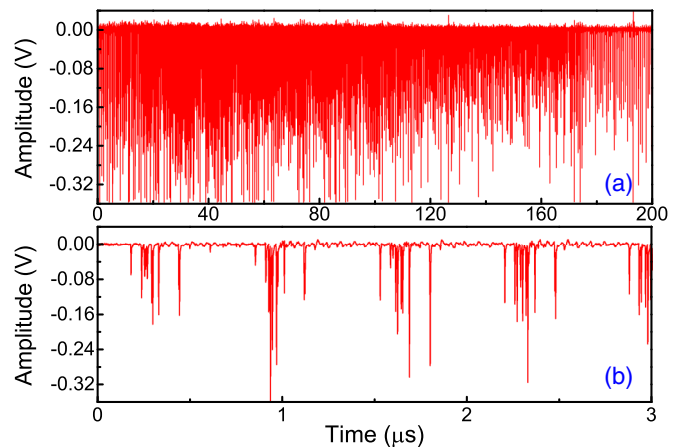


FIG. 1. An example of timing signals from the MCP detector recorded by the oscilloscope. The detector was switched on 33  $\mu\text{s}$  after the injection of ions into CSRe. The entire measurement of 200  $\mu\text{s}$  and a part of the spectrum zoomed on the first 3  $\mu\text{s}$  are illustrated in panels (a) and (b), respectively.

if the isochronous condition, namely  $\gamma = \gamma_i$ , is fulfilled. In the experiment,  $\gamma_i$  of CSRe was set to be 1.302, fulfilling the isochronous condition for  $^{94}\text{Ru}^{44+}$ .

The revolution times of stored ions were measured using a time-of-flight (ToF) detector [35] placed inside CSRe. The detector is equipped with a  $19\text{ }\mu\text{g}/\text{cm}^2$  carbon foil 40 mm in diameter. Secondary electrons were released from the foil when stored ions passed through it. They were guided isochronously to the microchannel plate (MCP) by the perpendicularly arranged electric and magnetic fields. The signals from the MCP were sampled with a digital oscilloscope Tektronix DPO 71254 at a sampling rate of 50 GHz. The recording time was 200  $\mu\text{s}$  for each injection, corresponding to  $\sim 300$  revolutions.

Since the magnetic rigidity acceptance of RIBLL2 is about one magnitude larger than that of CSRe, most of the ions injected into the CSRe could only survive a few revolutions before they were lost on the CSRe vacuum pipe. Such ions pass through the carbon foil of the ToF detector and release a huge number of secondary electrons, which in consequence discharge a large number of MCP channels. Therefore, a considerable saturation effect is caused by these “short-survival” ions, affecting the detection efficiency and signal amplitudes of the detector. In order to avoid discharging too many channels during the first few revolutions, a pulsed high-voltage power supply [36] was employed in this experiment. The detector was switched on 33  $\mu\text{s}$  after the injection. A typical signal sequence from one injection is presented in Fig. 1(a). Figure 1(b) shows an enlargement of the first several revolutions after the detector was turned on.

*Data analysis.* On average, about five ions were simultaneously stored in CSRe in one injection. The recorded signals—as shown in Fig. 1—were assigned to specific ions by using a periodic signal tracing algorithm [37,38], which is used in typical IMS experiments at CSRe [27–30]. The time stamps of each ion passing through the detector were fitted with a polynomial function of the revolution number.

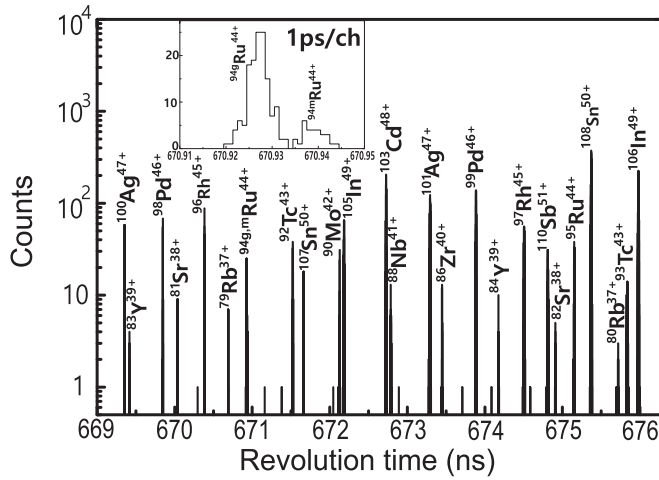


FIG. 2. The revolution time spectrum enlarged in a narrow time window of  $669.0 \text{ ns} \leq t \leq 676.5 \text{ ns}$ . The inset shows the well-resolved peaks of the ground (g) and isomeric (m) states of  $^{94}\text{Ru}$ . Identified decay events of  $^{94m}\text{Ru}$  were excluded from this spectrum.

The revolution time was determined from the slope of the fit curve at a given revolution number. The ion identification was realized by comparing the measured and simulated revolution time spectra, as done in our earlier works [27–30,38].

In the revolution time spectrum, obtained directly by accumulating the revolution times into a histogram, the isomer and the ground state of  $^{94}\text{Ru}$  cannot be resolved due to the instabilities of the magnetic fields. The latter cause shifts in revolution times for different injections. Exploiting the fact that several ions were stored in CSRe simultaneously and assuming the shifts are identical for all ions in one injection, we corrected the effects of the magnetic-field instabilities using the method described in Ref. [39]. The revolution time spectrum with an improved resolution was thus obtained. It is shown in Fig. 2, where the inset shows the well-separated two states of  $^{94}\text{Ru}$ . The identification of decay events of  $^{94m}\text{Ru}$  is described below. All observed decay events were excluded in Fig. 2.

By using the nuclides with well-known masses as calibrants, the mass excesses of the isomer and the ground state of  $^{94}\text{Ru}$  were determined to be  $-79905(132) \text{ keV}$  and  $-82531(72) \text{ keV}$ , respectively, in good agreement with the values of  $-79940(3) \text{ keV}$  and  $-82584(3) \text{ keV}$  from the latest Atomic Mass Evaluation, AME 2016 [32]. We note that our work represents the mass measurement of the shortest lived nuclear state using a storage ring.

From the excitation energy of  $^{94m}\text{Ru}$  and the optical setting of CSRe, the revolution time difference between the isomeric and ground states was calculated to be  $11.9 \text{ ps}$ . If the isomer decays during its circulation in CSRe, then the revolution time will decrease by  $\sim 11.9 \text{ ps}$ . This revolution time difference is much smaller than the intrinsic time resolution ( $\sim 50 \text{ ps}$ ) of the ToF detector used in this experiment [35]. Furthermore, due to the finite emittance of the ion [40], the revolution times at different revolutions may fluctuate with a magnitude of larger than  $100 \text{ ps}$ . To solve this challenge, a tolerance of  $220 \text{ ps}$  was introduced, which is similar to earlier experiments

[37,38]. The periodic signals were searched for within the range of tolerance, which is much larger than the revolution time difference caused by the decay. Therefore, even if a decay occurred during the storage time, it would not influence the proper assignment of the signals to the corresponding ion.

As discussed above, it was not possible to identify the decay of  $^{94m}\text{Ru}^{44+}$  by simply comparing the revolution times from consecutive signals of the adjacent turns, since the revolution time difference caused by the decay is much smaller than the time resolution of the ToF detector and the fluctuations due to the beam emittance. However, the uncertainty for the revolution time determination can largely be reduced by averaging the revolution times of several consecutive revolutions. In the data analysis, we found that the uncertainty originated from the time resolution of the ToF detector can be approximately described as

$$\delta T \approx 3.46\sigma / \sqrt{\eta N^3}, \quad (2)$$

where  $\eta$  is the detection efficiency of this measurement (roughly 80% for  $^{94m}\text{Ru}^{44+}$ ),  $\sigma$  is the time resolution of the detector, and  $N$  is the turn number used in the fitting. The uncertainty of the revolution time determination decreases as a function of turn number to the power of 1.5. By analyzing the simulated data [40], we found that the influence of the fluctuations due to the ion emittance on the determination of the revolution time can also be eliminated by averaging the data from a large number of revolutions. It was estimated that by using the data acquired in  $20 \mu\text{s}$ , the uncertainty of revolution time determination was  $\sim 2 \text{ ps}$ , which corresponds to a mass resolving power of  $\sim 8 \times 10^4$ , sufficient to identify the decay events. In such circumstances, the sensitive observation window was defined by subtracting  $20 \mu\text{s}$  at the beginning and the end of the  $200\text{-}\mu\text{s}$ -long data acquisition duration. Consequently, the effective time window is from  $20$  to  $180 \mu\text{s}$  after the start of the data acquisition. If a decay occurred outside of the observation window, the number of revolutions before or after the decay is too small to extract the revolution time with sufficient accuracy for an unambiguous identification, so the decay event was disregarded.

During the storage time, the revolution time of  $^{94g,m}\text{Ru}^{44+}$  is approximately constant despite the energy loss in the carbon foil of the detector thanks to the isochronous settings of CSRe. From the experimental conditions, all ions with revolution times in the range from  $670.90$  to  $670.98 \text{ ns}$  must be  $^{94g,m}\text{Ru}^{44+}$ . All observed  $^{94g,m}\text{Ru}^{44+}$  ions were considered in the decay search. For each of them, we fitted the time stamps acquired in every consecutive  $20\text{-}\mu\text{s}$  period using a linear function of the turn number and extracted the revolution time as the slope of the fit function in the corresponding time period. Thus, we obtained the revolution time as a function of revolution number. Two examples are shown in Figs. 3(a) and 3(b) with no-decay and decay events, respectively. The revolution time is approximately constant in Fig. 3(a), verifying the isochronous settings of CSRe. However, a sudden drop is observed in Fig. 3(b), which indicates an isomeric decay. The difference of the revolution times before and after the sudden

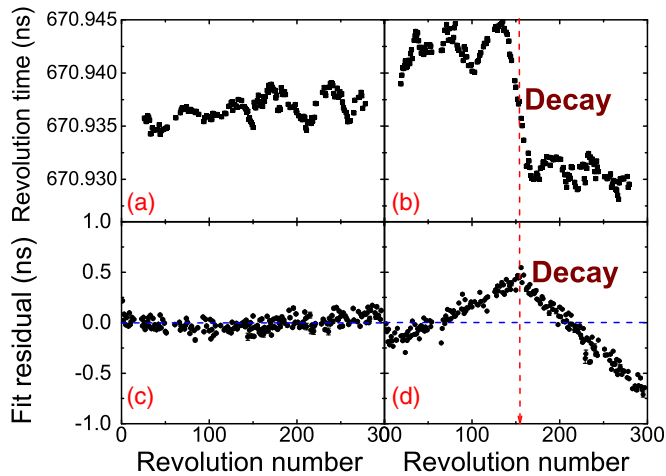


FIG. 3. The revolution time as a function of revolution number for no-decay (a) and decay (b) events. The residuals of the linear fit of the data for these two events are shown in panels (c) and (d), respectively. The vertical lines in panels (b) and (d) mark the decay time. Please note the significantly different scales in the upper and lower panels. The oscillation-like behavior seen in the upper panels may be due to the finite emittance of the beam [41,42].

drop is about 12 ps, corresponding to the excitation energy of the isomer. For each of the  $^{94g,m}\text{Ru}^{44+}$ , we also fitted all obtained revolution times with a linear function of the turn number. The residuals of the fitting are shown in Figs. 3(c) and 3(d) for the same two examples, respectively. There is no structure visible in the residual plot of Fig. 3(c). The scatter of the time stamps from the fit is within 220 ps, corresponding to the tolerance used in the algorithm for searching periodic signals. In Fig. 3(d), systematic deviations from the linear fit, which vary from  $-700$  to  $+500$  ps, are evident. A clear kink is visible, which points to a sudden change of the revolution time. This sudden change of the revolution time and the kink in the residual plot correspond to each other and are the signatures of an isomeric decay.

To extract the decay time, the data point with the largest positive deviation from the linear fit, corresponding to the kink, was chosen as the separation point. The time stamps before and after it were fitted separately with linear functions of the turn number. Then two straight lines were obtained and their intersection was determined as the decay time. The decay time is indicated in Figs. 3(b) and 3(d) with vertical line. According to simulations, the uncertainty for the decay time determination is smaller than  $1 \mu\text{s}$ . The accuracy is found to be maximal for decays occurring in the middle of the data acquisition time, where the number of data points is large on both sides of the decay time.

**Results and discussion.** The half-life of  $^{94m}\text{Ru}^{44+}$  has been obtained in two ways. In total we identified 49 decays in the observation window. From the decay times of these 49 events, the half-life of  $^{94m}\text{Ru}^{44+}$  was determined to be  $116(79) \mu\text{s}$ . The large uncertainty is due to the low statistics and the small observation window.

However, 37 of 49 valid decay events occurred in the injections in which the number of reference nuclides was

sufficient to perform the correction for the magnetic-field instabilities. Thus, a reliable assignment of each no-decay event could be done either to the ground or isomeric state of  $^{94}\text{Ru}$ . In the analysis, 29  $^{94m}\text{Ru}^{44+}$  ions were identified, which survived throughout the observation window; see the insert in Fig. 2. The lifetime of  $^{94m}\text{Ru}^{44+}$  and the corresponding uncertainty can be obtained from

$$\hat{\tau} = \frac{1}{n} \sum_{i=1}^n t_i - T_1 + \frac{m(T_2 - T_1)}{n}, \quad (3)$$

$$\sigma_{\hat{\tau}} = \frac{\hat{\tau}}{\sqrt{(n+m)(1 - e^{-(T_2-T_1)/\hat{\tau}})}}, \quad (4)$$

where  $(T_1, T_2)$  defines the observation window,  $n$  is the number of the decay events ( $n = 37$ ),  $t_i$  are the decay times, and  $m$  is the number of isomers that did not decay in the observation window ( $m = 29$ ). More details on the method for the lifetime estimation can be found in Ref. [43]. The half-life of  $^{94m}\text{Ru}^{44+}$  in the rest frame was determined to be  $102(17) \mu\text{s}$ . The uncertainty is mainly due to the low statistics and can be improved by accumulating more events.

From the half-life of  $^{94m}\text{Ru}^{44+}$ , the ICC was obtained to be  $0.44(24)$ , in agreement with the BRICC calculation [33]. The population ratio of the isomer in  $^{94}\text{Ru}$  after the production target was determined to be  $43(3)\%$ . This result can be important for the investigations of angular momentum population following the projectile fragmentation [44].

In conventional IMS experiments, the mass resolving power is mainly determined by the velocity spread of the stored ions in different injections. The instability of the magnetic fields is another significant constraint [37]. However, the uncertainty of the revolution time determination in one specific injection is only influenced by the time resolution of the ToF detector and the fluctuations caused by the emittance. In this experiment, the observation window was defined according to the required mass resolution, which was determined by the excitation energy of the isomer. The mass resolving power of  $\sim 8 \times 10^4$  was achieved here. Higher resolving power can be reached by averaging more revolutions, i.e., shrinking the observation window. If we define the observation window to be from  $50$  to  $150 \mu\text{s}$  after the data acquisition started, the data acquired in  $50\text{-}\mu\text{s}$  steps can be used. In this way, it was estimated that the resolving power of  $\sim 150\,000$  can be realized, which means that the decay of an isomer with excitation energy  $\sim 600 \text{ keV}$  in this mass region can be identified. However, with even more data used for averaging, the achievable resolving power would be limited by the imperfection of the isochronous settings [41,42].

**Summary.** In summary, the half-life and the mass of the fully stripped ion  $^{94m}\text{Ru}^{44+}$  have been measured using the isochronous mass spectrometry. The advantage of the IMS is that the revolution times of stored ions in a storage ring are measured in time intervals shorter than  $\mu\text{s}$ , and consequently it is sensitive enough to observe nuclear decays occurring on a time scale from a few  $\mu\text{s}$  to a few hundred  $\mu\text{s}$ . The decay of  $^{94m}\text{Ru}^{44+}$  was identified through a sudden mass change during the observation time. This work proved the feasibility to study the decays of short-lived isomers in highly charged ions by using IMS. Finally, it is worth noting that  $^{94m}\text{Ru}^{44+}$



is the shortest-lived nuclear state whose mass has ever been measured directly.

*Acknowledgements.* The authors are grateful to the HIRFL-CSR accelerator group for the help during the experiment. This work is supported in part by National Key Program for S&T Research and Development (Grant No. 2016YFA0400504); the Major State Basic Research Development Program of China (Contract No. 2013CB834401); the Key Research

Program of Frontier Sciences, CAS (Grant No. QYZDJ-SSW-S); NSFC Grants No. U1232208, No. U1432125, No. 11605248, No. 11605249, No. 11605252, and No. 11605267; the CAS Pioneer Hundred Talents Program; the Max-Planck Society; and the Helmholtz-CAS Joint Research Group HCJRG-108. Y.H.Z. acknowledges the support by the ExtreMe Matter Institute (EMMI) at the GSI Helmholtzzentrum für Schwerionenforschung, Darmstadt, Germany.

- 
- [1] W. R. Phillips, I. Ahmad, D. W. Banes, B. G. Glagola, W. Henning, W. Kutschera, K. E. Rehm, J. P. Schiffer, and T. F. Wang, *Phys. Rev. Lett.* **62**, 1025 (1989).
- [2] M. Jung, F. Bosch, K. Beckert, H. Eickhoff, H. Folger, B. Franzke, A. Gruber, P. Kienle, O. Klepper, W. Koenig *et al.*, *Phys. Rev. Lett.* **69**, 2164 (1992).
- [3] F. Attallah, M. Aiche, J. F. Chemin, J. N. Scheurer, W. E. Meyerhof, J. P. Grandin, P. Aguer, G. Bogaert, J. Kiener, A. Lefebvre *et al.*, *Phys. Rev. Lett.* **75**, 1715 (1995).
- [4] H. Imrich, H. Geissel, F. Nolden, K. Beckert, F. Bosch, H. Eickhoff, B. Franzke, Y. Fujita, M. Hausmann, H. C. Jung *et al.*, *Phys. Rev. Lett.* **75**, 4182 (1995).
- [5] F. Bosch, T. Faestermann, J. Friese, F. Heine, P. Kienle, E. Wefers, K. Zeitelhack, K. Beckert, B. Franzke, O. Klepper *et al.*, *Phys. Rev. Lett.* **77**, 5190 (1996).
- [6] Yu. A. Litvinov, F. Attallah, K. Beckert, F. Bosch, D. Boutin, M. Falch, B. Franzke, H. Geissel, M. Hausmann, Th. Kerscher *et al.*, *Phys. Lett. B* **573**, 80 (2003).
- [7] T. Ohtsubo, F. Bosch, H. Geissel, L. Maier, C. Scheidenberger, F. Attallah, K. Beckert, P. Beller, D. Boutin, T. Faestermann *et al.*, *Phys. Rev. Lett.* **95**, 052501 (2005).
- [8] Y. A. Litvinov, F. Bosch, H. Geissel, J. Kurcewicz, Z. Patyk, N. Winckler, L. Batist, K. Beckert, D. Boutin, C. Brandau *et al.*, *Phys. Rev. Lett.* **99**, 262501 (2007).
- [9] Y. A. Litvinov *et al.*, *Phys. Lett. B* **664**, 162 (2008).
- [10] Y. A. Litvinov and F. Bosch, *Rep. Prog. Phys.* **74**, 016301 (2011).
- [11] P. Kienle *et al.*, *Phys. Lett. B* **726**, 638 (2013).
- [12] A. Akber, M. W. Reed, P. M. Walker, Y. A. Litvinov, G. J. Lane, T. Kibedi, K. Blaum, F. Bosch, C. Brandau, J. J. Carroll *et al.*, *Phys. Rev. C* **91**, 031301 (2015).
- [13] J. N. Bahcall, *Phys. Rev.* **126**, 1143 (1962).
- [14] Y. H. Zhang *et al.*, *Phys. Scr.* **91**, 073002 (2016).
- [15] A. Lennarz, A. Grossheim, K. G. Leach, M. Alanssari, T. Brunner, A. Chaudhuri, U. Chowdhury, J. C. Lopez-Urrutia, A. T. Gallant, M. Holl *et al.*, *Phys. Rev. Lett.* **113**, 082502 (2014).
- [16] B. Franzke *et al.*, *Mass Spectr. Rev.* **27**, 428 (2008).
- [17] Y. A. Litvinov *et al.*, *Nucl. Phys. A* **734**, 473 (2004).
- [18] Y. A. Litvinov *et al.*, *Nucl. Phys. A* **756**, 3 (2005).
- [19] M. W. Reed, I. J. Cullen, P. M. Walker, Y. A. Litvinov, K. Blaum, F. Bosch, C. Brandau, J. J. Carroll, D. M. Cullen, A. Y. Deo *et al.*, *Phys. Rev. Lett.* **105**, 172501 (2010).
- [20] L. Chen, P. M. Walker, H. Geissel, Y. A. Litvinov, K. Beckert, P. Beller, F. Bosch, D. Boutin, L. Caceres, J. J. Carroll *et al.*, *Phys. Rev. Lett.* **110**, 122502 (2013).
- [21] B. Sun *et al.*, *Eur. Phys. J. A* **31**, 393 (2007).
- [22] M. Hausmann *et al.*, *Nucl. Instrum. Meth. A* **446**, 569 (2000).
- [23] M. Hausmann *et al.*, *Hyperfine Interact.* **132**, 291 (2001).
- [24] B. Sun *et al.*, *Phys. Lett. B* **688**, 294 (2010).
- [25] B. Sun *et al.*, *Nucl. Phys. A* **812**, 1 (2008).
- [26] R. Knöbel *et al.*, *Eur. Phys. J. A* **52**, 138 (2016).
- [27] X. L. Tu, H. S. Xu, M. Wang, Y. H. Zhang, Y. A. Litvinov, Y. Sun, H. Schatz, X. H. Zhou, Y. J. Yuan, J. W. Xia *et al.*, *Phys. Rev. Lett.* **106**, 112501 (2011).
- [28] Y. H. Zhang, H. S. Xu, Y. A. Litvinov, X. L. Tu, X. L. Yan, S. Typel, K. Blaum, M. Wang, X. H. Zhou, Y. Sun *et al.*, *Phys. Rev. Lett.* **109**, 102501 (2012).
- [29] X. Xu, P. Zhang, P. Shuai, R. J. Chen, X. L. Yan, Y. H. Zhang, M. Wang, Y. A. Litvinov, H. S. Xu, T. Bao *et al.*, *Phys. Rev. Lett.* **117**, 182503 (2016).
- [30] P. Zhang *et al.*, *Phys. Lett. B* **767**, 20 (2017).
- [31] D. Abriola and A. A. Sonzogni, *Nucl. Data Sheet* **107**, 2423 (2006).
- [32] G. Audi *et al.*, *Chin. Phys. C* **41**, 030001 (2017).
- [33] T. Kibédi *et al.*, *Nucl. Instrum. Meth. A* **589**, 202 (2008).
- [34] J. W. Xia *et al.*, *Nucl. Instrum. Meth. A* **488**, 11 (2002).
- [35] B. Mei *et al.*, *Nucl. Instrum. Meth. A* **624**, 109 (2010).
- [36] W. Zhang *et al.*, *Nucl. Instrum. Meth. A* **755**, 38 (2014).
- [37] R. J. Chen *et al.*, *JPS Conf. Proc.* **14**, 021101 (2017).
- [38] X. L. Tu *et al.*, *Nucl. Instrum. Meth. A* **654**, 213 (2011).
- [39] P. Shuai *et al.*, *arXiv:1407.3459*.
- [40] R. J. Chen *et al.*, *Phys. Scr. T* **166**, 014044 (2015).
- [41] S. Litvinov *et al.*, *Nucl. Instrum. Meth. A* **724**, 20 (2013).
- [42] A. Dolinskii *et al.*, *Nucl. Instrum. Meth. A* **574**, 207 (2007).
- [43] X. C. Chen, Q. Zeng, Yu. A. Litvinov, X. L. Tu, P. M. Walker, M. Wang, Q. Wang, K. Yue, and Y. H. Zhang, *Phys. Rev. C* **96**, 034302 (2017).
- [44] X. L. Tu, A. Kelic-Heil, Y. A. Litvinov, Z. Podolyak, Y. H. Zhang, W. J. Huang, H. S. Xu, K. Blaum, F. Bosch, R. J. Chen *et al.*, *Phys. Rev. C* **95**, 014610 (2017).